EFFECTS OF HYDROGEN CONTENT, TEMPERATURE, AND CRACK CONFIGURATION ON FATIGUE CRACK PROPAGATION AND UNSTABLE FRACTURE BEHAVIOUR OF Zr-2.5Nb PRESSURE TUBE

S. KUSUMOTO, A. NISHIOKA, H. MAKI, S. USAMI
Hitachi Research Laboratory, Hitachi, Ltd., Saiwai-machi, Hitachi-shi, Japan

K. HAYASHI
Advanced Thermal Reactor Project,
Power Reactor and Nuclear Fuel Development Corp., Minato-ku, Tokyo, Japan

Y. ANDO
Department of Nuclear Engineering,
University of Tokyo, Bunkyo-ku, Tokyo, Japan

SUMMARY

The unstable fracture behaviour was studied on the Zr-2.5Nb pressure tube intended to be used in the heavy water moderated and light water cooled reactor, "FUGEN", from the viewpoints of the effect of hydrogen content, temperature and crack configuration. The test methods are as follows: (1) the internally pressurizing test on the pressure tube, (2) the ring tensile test and (3) the bending test using a small crescentshaped specimen. The methods (2) and (3), were developed in anticipation of their usefulness for surveillance of the pressure tube material served in the reactor.

The hydrogen content of the specimens was ranged from 5 to 300 ppm, the test temperature was changed from a room temperature to 300°C and the various crack configurations, that is, the different sizes in length and depth were studied. The effects of these parameters were observed from the viewpoints of the fracture strength, the number of cycles to crack initiation, the fatigue crack growth rate and the fracture behaviour.

The results were examined by application of the linear fracture mechanics, and under small scale yielding condition, the effects of the difference of the test methods ((1), (2) and (3)) could be eliminated by using the stress intensity factor.

The stress intensity factor of the specimen with a part through crack under internal pressure was obtained semi-experimentally, and the two-dimensional fatigue crack growth rate was elucidated by using this stress intensity factor. As the result, it was clarified that the behaviour of a part through crack versus the above stress intensity factor agreed well with the behaviour of a through crack.

At room temperature, such high hydrogen content as 250 ppm makes the fracture toughness decrease extremely and makes the fatigue crack growth rate increase prominently as, Kmax approaches to Kc. However, the fracture toughness has recovered at 300°C.

On the other hand, it was confirmed that pre-loading at a high temperature is effective to improve the fracture toughness at a room temperature.

1. Introduction

The Power Reactor and Nuclear Fuel Development Corporation has been developing the prototype reactor, "FUGEN", heavy water moderated and light water boiling cooled. It was decided that the aged Zr-2.5Nb was adopted as the pressure tube material because of its good nuclear characteristics and its high mechanical strength.

Hydrogen picked up from the coolant water and neutron irradiation reportedly lead to embrittement of the pressure tube. One of the most severe assumptions is the accident that terminates in unstable fracture of the pressure tube after crack initiation at a small defect and its propagation by pressure cycling resulted from start-up and shut-down of the reactor.

This program was planned to study the fracture behaviour of the aged Zr-2.5Nb, that is, the effects of repeated stress, two-dimensional crack configuration, hydrogen content and temperature on the crack growth rate, the fracture toughness and the fracture mode. Additionally, pre-loading at a high temperature was tried to improve the toughness at a room temperature.

The present study consists mainly of three experiments, that is, the tube pressurizing test, the ring tensile test and the bending test. These tests were performed on the pressure tube satisfying the specifications for the prototype reactor. It is expected that the reliable results are obtained by the tube pressurizing test, because it is performed on large specimens. On the other hand, the ring tensile and the bending tests are useful as the methods for surveillance of the pressure tube served in the reactor, if the correlation between their results and the results of the tube pressurizing test is successfully made clear.

2. Experimental Techniques

2.1 Material

The investigated material is the aged extruded tube made from Zr-2.5Nb satisfying the specifications for the pressure tube of the reactor. The heat treatment consisted of water quenching from 870°C, cold drawn to a reduction of 10 ~ 15% and then given an aging treatment which consisted of holding at 500°C in vacuum for 24 h. Its dimensions are 117.8 mm in inside diameter and 4.3 mm in wall thickness. Four kinds of specimen were prepared differently in hydrogen content aimed at 5 (as received), 50, 100 and 250 ppm. Hydrogen was charged by the following method : a 800 mm long piece was shot blasted on the surface and heated at 450 ~ 500°C in hydrogen gas for a few hour.

Table I shows the circumferential mechanical properties of the material measured by the ring tensile test using 6.4 mm wide ring pieces (Kimura [1]). The effects of hydrogen content on the mechanical properties are not so prominent.

2.2 Tube Pressurizing Test

Figure 1 shows schematically the construction of the specimen and the end fixtures for the tube pressurizing test, (Pankaskie [2]).

The 0.3 mm wide notch was longitudinally added through or part through the wall thickness at the middle part of the 500 mm long piece by means of the electrical discharge machining method. The through notch was sealed with 0.1 mm thick copper foil and 2 mm thick rubber sheet stuck with plastic paste.

The specimen is connected at the both ends with the end fixtures through one of which high pressure silicon oil is supplied. The delta packings seal the passage of high pressure silicon oil and the wedge shaped chacks catch the tubular specimen on the outside surface against the axial force induced by the internal pressure.

A few specimens were supplied to the static burst test directly after notch machining and others were after the fatigue cracked. The static burst test at high temperature was performed on the specimen with the heater inside and wrapped outside with thermal insulator.

In the case of the fatigue test, internal pressure cycling with 2 kg/mm^2 as the lower stress was continued until the specimen fractured. The crack behaviour such as initiation and propagation was observed with a microscope.

2.3 Ring Tensile Test

Such a method was developed to reproduce the similar stress conditions in a ring specimen as those in a tubular specimen under internal pressure.

The specimen is a 100 mm long piece of tubing and it is added a narrow notch in the same manner as mentioned in 2.2. The specimen is set on the tensile testing machine with

a pair of semi-cylindrical jigs that is spaced from the internal surface of the specimen with teflon sheet to reduce friction force, as shown in Fig. 2. The notch is located at 45° in the angle of elevation from the horizontal plane to minimize the out of plane bending at the notch area and also to make observation easier. It was certified by the preliminary test using the non-notched specimen instrumented with strain gauges that stress distributed uniformly in the longitudinal direction of tubing. The stress distribution of each specimen was monitored by three strain gauges stuck at both ends and the middle of the length and the uniformity was kept within ±5% by adjustment in setting the jigs and the specimen.

The specimen was applied pulsating tensile stress until fatigue cracks were made to propagate a few millimeters at the notch tips. Static tensile load was increased until the specimen fractured after crack formation had been interrupted.

In the case of the fatigue test, application of pulsating tensile stress with 2 kg/mm^2 as the lower stress was continued until the specimen fractured. The crack behaviour was observed by the same way as mentioned in 2.2 and in the high temperature test through the window furnished on the furnace.

2.4 Bending Test

The special bending test was developed as the method for surveillance of the pressure tube served in the reactor.

The crescent-shaped specimen is cut from the pressure tube, with dimensions of 75 mm in circumferencial length, 30 mm wide and 4.3 mm thick. A sharp notch is cut at the middle on the transverse cross section. As shown in Fig. 3, the specimen is set at both ends on the jig inclining by 13.5° from the load axis to avoid the out of plane bending at the notch area.

Pulsating bending load was applied to the specimen to make a fatigue crack at the root of the notch by three points bending. Afterward, static bending force was increased until the specimen fractured to obtain the fracture toughness.

3. Results and Discussion

3.1 Stress Intensity Factor

Stress intensity factor, K, was used for the data arrangement, since both the stress range in the fatigue test and the static fracture stress were sufficiently low, in general, compared with the 0.2% offset were sufficiently low, in general, compared with the 0.2% offset yield strength. The following equations give the values of stress intensity factor.

Tubular specimen with a through crack under internal pressure (Erdogan & Kibler [3])

$$K = I\sigma\sqrt{\pi a} \tag{1}$$

Tubular specimen with a infinite long and part-through crack under internal pressure (Kobayashi, et al. [4])

$$K = F\sigma\sqrt{\pi a} \tag{2}$$

Ring tensile specimen with a through crack (lets use the equation for the plate specimen with a through crack under tensile load) (Feddersen [5])

$$K = \sigma_n \left(1 - \frac{2a}{W}\right)\sqrt{\pi a \sec\frac{\pi a}{W}} \tag{3}$$

Ring tensile specimen with part-through crack (lets use the equation for the plate specimen with semi-elliptical crack under tensile load) (Kobayashi & Moss 6)

$$K = N\sigma_g\sqrt{\pi a/Q} \tag{4}$$

Three points bending specimen (Brown & Srawley [7])

$$K = \sigma_g\sqrt{a}\left[1.93-3.07\left(\frac{a}{H}\right)+14.53\left(\frac{a}{H}\right)^2-25.11\left(\frac{a}{H}\right)^3+25.80\left(\frac{a}{H}\right)^4\right] \tag{5}$$

where

a	:	half length of a through crack or depth of the part-through crack
I,F	:	coefficients representing buldge effect
N	:	coefficient representing thickness effect
Q	:	coefficient representing effect of two-dimensional crack configuration
σ_n	:	net section stress
σ_g	:	gross stress

The gross stress in eq. (5) is expressed as follows,

$$\sigma_g = 6\ M \cos\theta / TH^2 \qquad (6)$$

where

M : in plane bending moment
T : thickness
H : width
θ : inclination angle

The stress intensity factor for the tubular specimen with a finite long and part-through crack under internal pressure will be afterwards discussed.

3.2 Unstable Fracture Behaviour

3.2.1 Effect of notch root configuration

In order to study the effects of notch root configuration, the static burst test was conducted on specimens with three kinds of notch of which roots were fatigue cracked, electrical discharge machined and drilled. The hydrogen content of the specimen was 250 ppm and the test temperature was room temperature.

Figure 4 shows the results. There is little difference between the specimens notched by electrical discharge machining and drilling. The fracture strength is approximately proportional to the square root of notch width (or the square root of radius of curvature at notch root). It means that the specimen fractures when the stress at the notch root attains at the critical value. The specimen with a fatigue crack is desirable to obtain Kc value for the case that the material fractures at low stress.

3.2.2 Effect of crack length on burst strength

Figure 5 shows the unstable burst strength at room temperature of the tubular specimens containing about 5 (as received) and 250 ppm hydrogen with through cracks. There scarcely observed any difference in strength between static burst and fatigue fracture. The fracture strength is well shown versus crack length by eq. (1) in which K is replaced by constant, the critical stress intensity factor, Kc ($350\ kg/mm^2\sqrt{mm}$ for the as-received material, $70\ kg/mm^2\sqrt{mm}$ for the material containing 250 ppm hydrogen). It shows that the linear fracture mechanics is useful in this case.

3.2.3 Effects of hydrogen content and test methods

Figure 6 shows the critical stress intensity factors, Kc, measured at room temperature by the various test methods versus hydrogen content. Their data are plotted within the band shown in the figure and the difference among the results by various methods is not recognized. The fracture toughness of the specimen containing 250 ppm hydrogen is about 1/5 of that of the specimen containing a little hydrogen. This is believed to be caused by microscopic fractures at brittle hydrides.

However, the values of Kc are apparently lower only in the case of the bending test on the specimens containing a little hydrogen (as-received), since they show the ductile facture behaviour. It is because a small specimen can not stand the higher stress than that for plastic hinge deformation. In this case, other approach, for example, the elastic-plastic fracture mechanics using such concept as the critical crack openning displacement is necessary to understand the fracture behaviour.

3.2.4 Effects of temperature

Figure 7 shows the tube burst strength versus crack length at 300°C. The fracture toughness has recovered completely and is not affected by hydrogen content at 300°C. The fracture behaviour with large bulge deformation also shows the ductile properties at 300°C even in case of specimens containing much hydrogen, though the macroscopic deformation is scarcely observed at room temperature. The strength of the cracked specimen approaches to that of the notched specimen in case of ductile fracture as shown in the figure, since the stress for ductile crack initiation becomes relatively higher than the stress for crack propagation (refer to the strength of the non-hydrided specimen in Fig. 5).

Figure 8 shows the effects of temperature on the fracture toughness. The fracture toughness of the specimen containing about 5 ppm decreases gradually with increasing temperature. However, in the case of the specimens containing 100 and 250 ppm hydrogen, the fracture toughness is about 1/2.5 and 1/5 of that of the specimen containing about 5 ppm hydrogen at a room temperature, recovers at 100 ~ 250°C rapidly and attains to the value

of the non-hydrided specimen at 300°C.

3.2.5 Pre-loading effects

Figure 9 shows the effects of pre-loading at 300°C on the increase in fracture toughness at a room temperature of the ring tensile specimen that contains 250 ppm hydrogen. The effect of the pre-loading depends on the manner of cooling and unloading, but the pre-loaded specimen is able to stand at a room temperature at least the load applied at 300°C. The present experiment shows the increase in fracture toughness by three times of the specimen without pre-loading. The pre-loading effects must be resulted by combination of the following phenomena : the large deformation in a small area at the crack tips and yielding in a comparatively large area that are caused by the large pre-stressing at a high temperature, and the compressive residual stress at the crack tips brought during unloading.

3.3 Stress Intensity Factor in Tubular Specimen with Semi-Elliptical Surface Crack Under Internal Pressure

It was tried to clarify semi-experimentally the stress intensity factor in the tubular specimen with a semi-elliptical part through crack under internal pressure. Figure 10 shows the tensile strength at room temperature of the ring specimen containing 250 ppm hydrogen. The calculated curve in Fig. 10 is obtained by eq. (4) in which the critical fracture toughness, Kc, is replaced by the constant, 70 $kg/mm^2\sqrt{mm}$. The experimental results agree well with the calculated curve as shown in the figure. It is conceivable from the above result that the fracture toughness in the radial direction of tubing is almost same as that in the longitudinal direction.

Figure 11 shows the examples of the fracture surfaces of the tube burst specimens containing 250 ppm hydrogen tested at a room temperature. The initial cracks added on these specimens were all 20 mm long but different in depth. The stress intensity factor of the part-through crack just before penetration is close to that of the through crack shown at the top of Fig. 11. Figure 12 shows the burst strength at room temperature of the tubular specimen containing 250 ppm hydrogen with a part-through crack. In case of the specimen with the part-through crack on the internal surface, the values shown in the figure are the sum of internal pressure and hoop stress. The contribution to stress intensity factor of the wedge effect amounts to about 14 percent of that of the hoop stress. With this treatment, it seems that there is no large difference in stress intensity factor between the part through cracks on the outside and the inside surfaces. The calculated curve shown in Fig. 12 was obtained by eq. (1) for the through crack, by eq. (2) for the infinite long and part through crack and by connecting the results of eqs. (1) and (2) considering the calculated results for the ring tensile shown in Fig. 10 and the experimental results of the tube burst test shown in Fig. 12.

Figure 13 shows the stress intensity factors obtained from the results shown in Figs. 10 and 12. It is found that the stress intensity factor for the tubular specimen increases due to the bulge effect, as compared with ring tensile specimen, with the increase of the ratio, crack depth or crack length to wall thickness.

3.4 Initiation and Propagation of Fatigue Crack

The correlation was studied between the number of cycles to crack initiation, Ni, at which crack grew about 0.1 mm and the range of the stress intensity factor, ΔKi, based on the assumption that the initial notch had been regarded as a crack instead of the true stress range at the notch tip. The correlation at a room temperature is shown in Figure 14. It shows that the effects of the mechanical parameters such as length of the through crack, two-dimentional configuration of the part through crack, stress range and test methods can be expressed by ΔKi. There is no effect of hydrogen content on fatigue crack initiation.

Figure 15 shows the correlation at a room temperature between the fatigue crack growth rate and the range of the stress intensity factor, ΔK. Accompanying crack extension the growth rate increases steeply as Kmax. approaches to Kc determined by hydrogen content and at last the specimens terminate at fracture, though in the case of small ΔK, the effect of hydrogen content on the growth rate is not observed. The fracture surface consists of the mixture of the white stripes formed by fatigue fracture and the black spots formed by brittle fracture as shown in Fig. 16. This was also confirmed by the electron micro-fractrography. The growth rate is in proportion to the cyclic plastic zone size or the cyclic crack openning displacement at a crack tip that is, nearly to ΔK^2 (OHUCHIDA, et al. [8] & [9]). The growth rate decreases rapidly with the decrease of ΔK, since ΔK approaches the threshold range, ΔKth, that is caused by the grain boundary impediment against the growth (OHUCHIDA, et al. [8]).

Figure 17 shows the fatigue crack growth rate at 300°C. The growth rate is not a affected by hydrogen at 300°C because the fracture toughness is not. The higher growth rate at 300°C than that at room temperature in case of small ΔK might be caused by lowering of ΔK_{th}.

Figure 18 shows the examples of the two-dimensional growth behaviour of the part-through cracks observed at 300°C. The beach mark shown in the figure was formed by the intermittent loading of small stress cycling. The growth behaviour of the part through crack on the ring and tube fatigue specimens agrees well by using the stress intensity factor obtained in Fig. 13 with that of the through crack as shown in Figs. 15 and 17.

4. Conclusions

(1) The fracture toughness decreases at room temperature with increase of hydrogen content. For example, the fracture toughness of the material containing 250 ppm hydrogen is about 1/5 of that of the material containing a little hydrogen (~5 ppm).

(2) The fracture toughness of the material containing 250 ppm hydrogen recovers steeply at 100 ~ 250°C and attains to the same value as that of the material containing a little hydrogen (~5 ppm), that is, the five times of that at a room temperature.

(3) The room temperature strength of the specimen pre-loaded at a high temperature increases at least up to the pre-stressed level.

(4) Though there is no effect of hydrogen content on the number of cycles to crack initiation and on the growth rate of the fatigue crack in case of small Kmax, the growth rate increases accompanying microscopic brittle fracture as Kmax approaches to Kc determined by hydrogen content.

(5) The growth rate of the fatigue crack at 300°C is a little higher than that at a room temperature in the case of small ΔK, but is lower in the case of large ΔK because of its recovery in toughness.

(6) The stress intensity factor was obtained semi-experimentally for the tubular specimen with a semi-elliptical part-through crack under internal pressure. It was clarified that by using this stress intensity factor the behaviour of a part through crack such as fracture mode and two-dimensional growth rate agree well with that of a through cracked specimen.

(7) It was confirmed that the ring tensile and the bending tests developed in the present study are able to simulate the behaviour of tubing under internal pressure and are useful for surveillance of the pressure tube serve in the reactor.

Acknowledgement

The authers wish to acknowledge advantageous pieces of advice and support of Prof. T. Udoguchi of Tokyo Univ., Mr. M. Akebi and Mr. S. Sawai of Power Reactor and Nuclear Fuel Development Corporation, Dr. Y. Fukuda of Hitachi Research Laboratory and Mr. E. Shibato of Hitachi Works. We are grateful to Mr. T. Aoki and co-works of Tokai Works of P.N.C. for supplying hydrided pressure tubes. The author was favored with the assistance of Mr. M. Watahiki.

References

[1] KIMURA, K., et al., Report of Japan Power Reactor and Nuclear Fuel Development Corp. No. SJ355 71-01 (1972)

[2] PANKASKIE, P. J., "Crack Propagation Characteristics of Zr-2.5wt%Nb Alloy Tubing" BNWL-560, Pacific Northwest Laboratory, Richland, Washigton (1967)

[3] ERDOGAN, F., KIBLER, J. J., "Cylindrical and Spherical Shells with Cracks", Inst. J. Fracture Mech. 5, 229 (1969)

[4] KOBAYASHI, A. S., et al., "Application of Finite Element Analysis Method to Two-Dimensional Problems on Fracture Mechanics" ASME Paper 69-WA/PVP-12 (1969)

[5] FEDDERSEN, C. E., "Discussion to Plane Strain Crack Toughness Testing of High Strength Metallic Materials", ASTM STP 410,77 (1967)

[6] KOBAYASHI, A. S., MOSS, W. L., "Stress Intensity Magnification Factors for Surface-Flawed Tension Plate and Round Tension Bar" Proc. 2nd Intern. Conf. on Fracture, Brighton, 31 (1969)

[7] BROWN, W. F., SRAWIEY, J. E., "Plane Strain Crack Toughness Testing of High Strength Metallic Materials" ASTM STP 410 (1967)

[8] OHUCHIDA, H., NISHIOKA, A., USAMI, S., "Elastic-plastic Appeoach to Fatigue Crack Propagation and Fatigue Limit of Materials with Crack" Preprint of 3rd Intern. Conf. on Fracture, München (1973)

[9] OHUCHIDA, H., NISHIOKA, A., USAMI, S., "Low Cycle Fatigue Behaviour of Spherical Pressure Vessel with Inclined Nozzle" IIW Doc. XIII-619-71 (1971)

Table I Circumferencial Mechanical Properties of Aged Zr-2.5Nb Tubing

TEMPERATURE (°C)	HYDROGEN CONTENT (ppm)	ULTIMATE STRENGTH (kg/mm^2)	0.2% PROOF STRESS (kg/mm^2)	ELONGATION (%)	REDUCTION IN AREA (%)
R.T.	0	87.7	79.4	18.8	48.5
	50	79.7	69.8	13.7	43.3
	300	73.6	62.7	12.1	32.4
300	0	59.7	—	18.0	64.0
	50	52.7	—	27.3	64.5
	100	52.3	—	21.1	63.0
	300	49.6	—	15.3	59.3

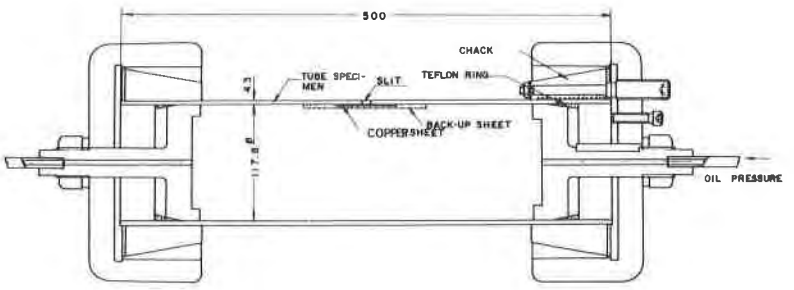

Fig. 1 Construction of Specimen Assembly for Tube Pressurizing Test

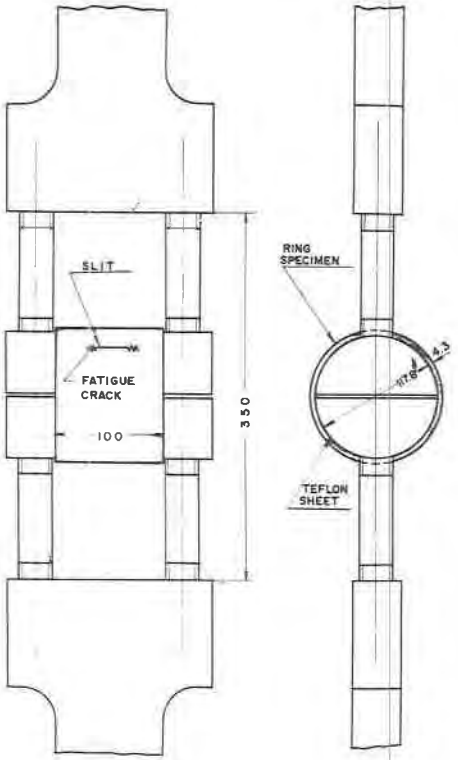

Fig. 2 Construction of Specimen Assembly for Ring Tensile Test

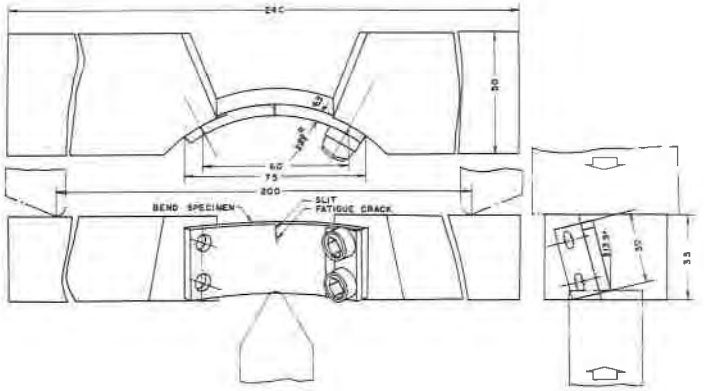

Fig. 3 Construction of Specimen Assembly for Bending Test

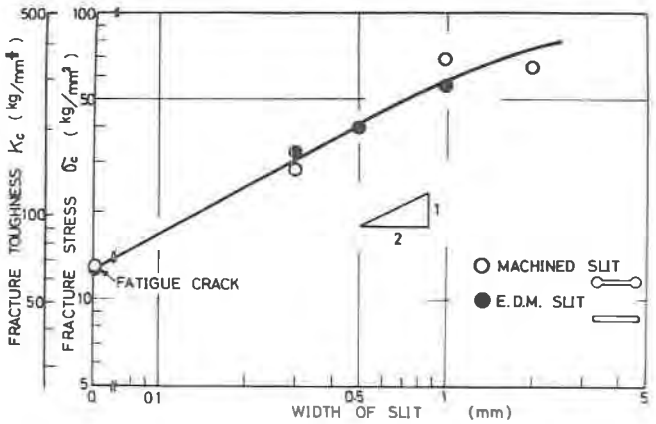

Fig. 4 Effect of notch root configuration on unstable fracture strength (ring tensile, 2a=35mm, hydrogen content: 250ppm, tested at room temperature)

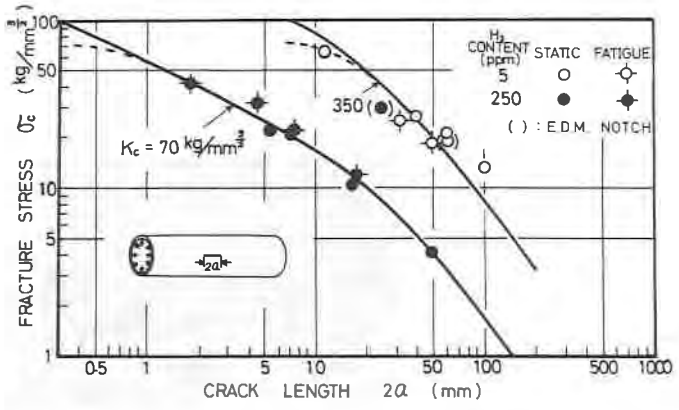

Fig. 5 Effect of crack length on tube burst strength (tested at room temperature)

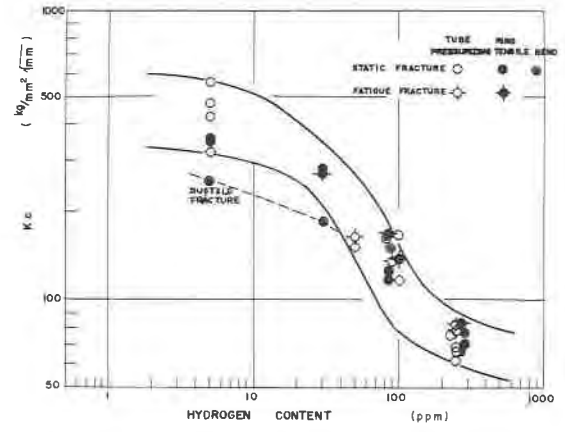

Fig. 6 Effect of hydrogen content and test methods on fracture toughness (tested at room temperature)

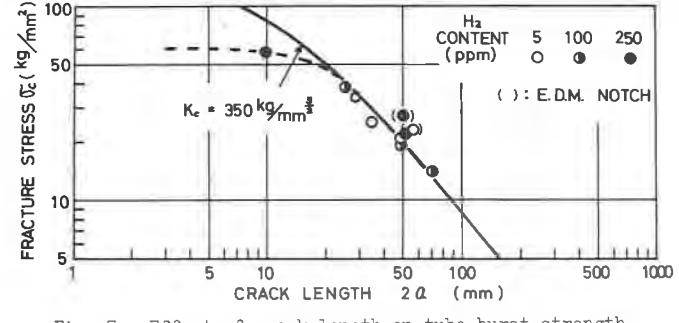

Fig. 7 Effect of crack length on tube burst strength (tested at 300°C)

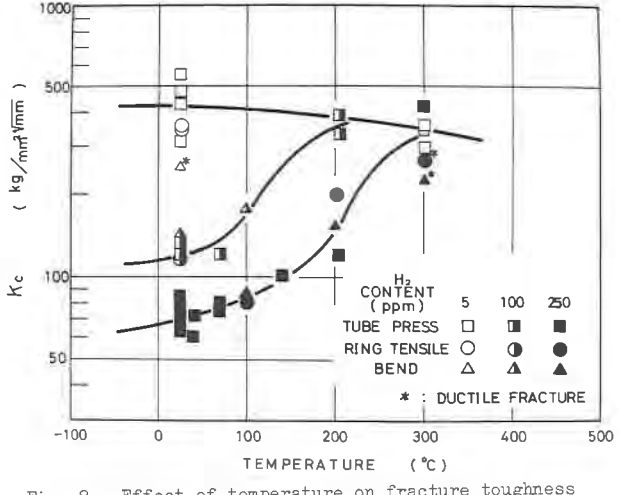

Fig. 8 Effect of temperature on fracture toughness

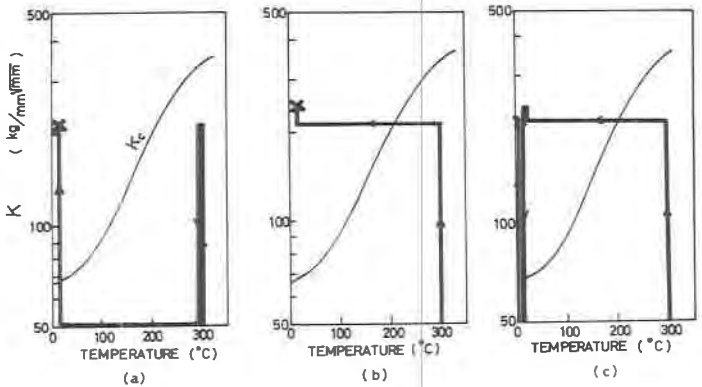

Fig. 9 Effects of pre-loading at high temperature on increase in fracture toughness at low temperature (ring tensile, 2a=35mm, hydrogen content: 250ppm)

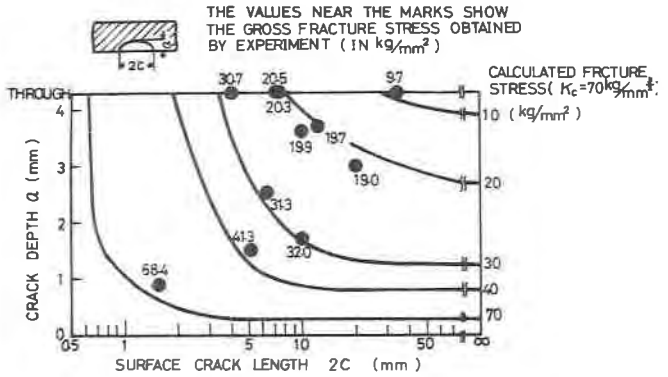

Fig. 10 Fracture Strength of Ring Tensile Specimen with Part Through Crack (hydrogen content: 250ppm)

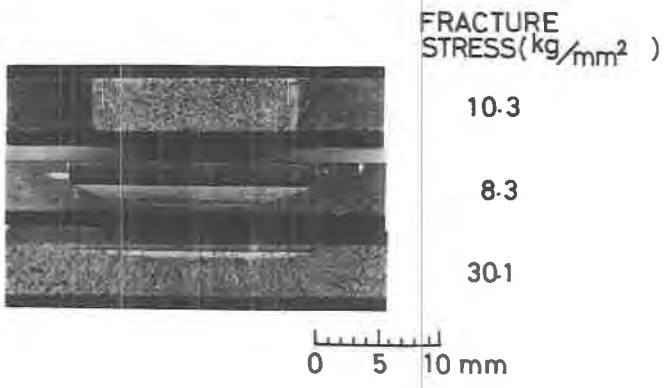

Fig. 11 Examples of Fracture Surfaces of Tube Burst Specimens (hydrogen content: 250ppm, tested at room temperature)

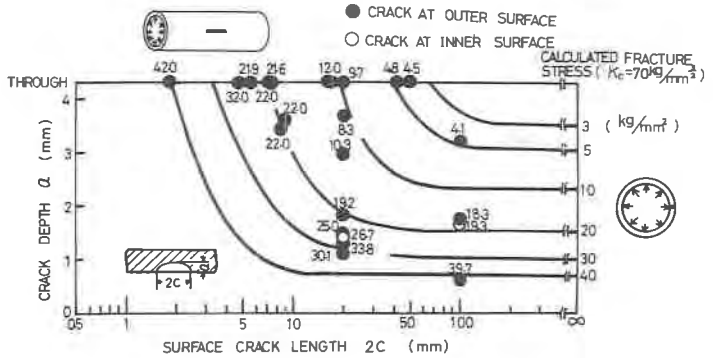

Fig. 12 Fracture Strength of Tube Burst Specimen with Part Through Crack (hydrogen content: 250ppm, tested at room temperature)

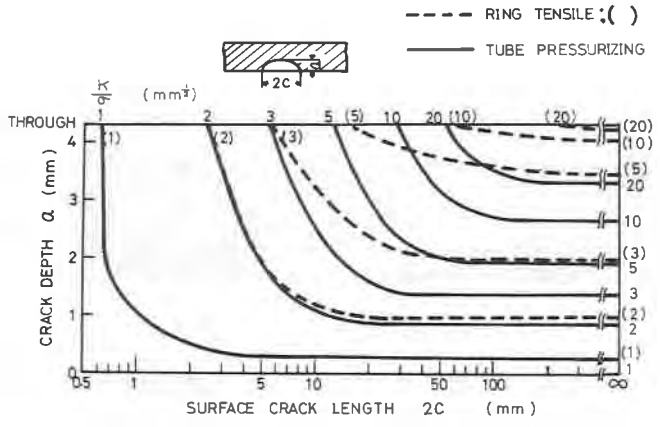

Fig. 13 Stress Intensity Factor of Tubular Specimen with Semi-Elliptical Crack under Internal Pressure

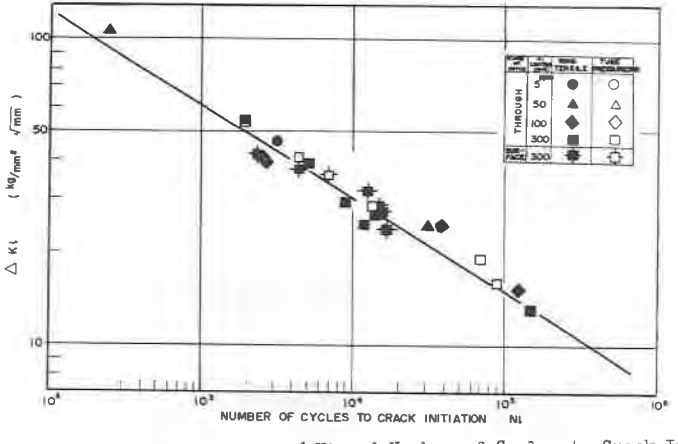

Fig. 14 Correlation between Δ Ki and Number of Cycles to Crack Initiation (tested at room temperature)

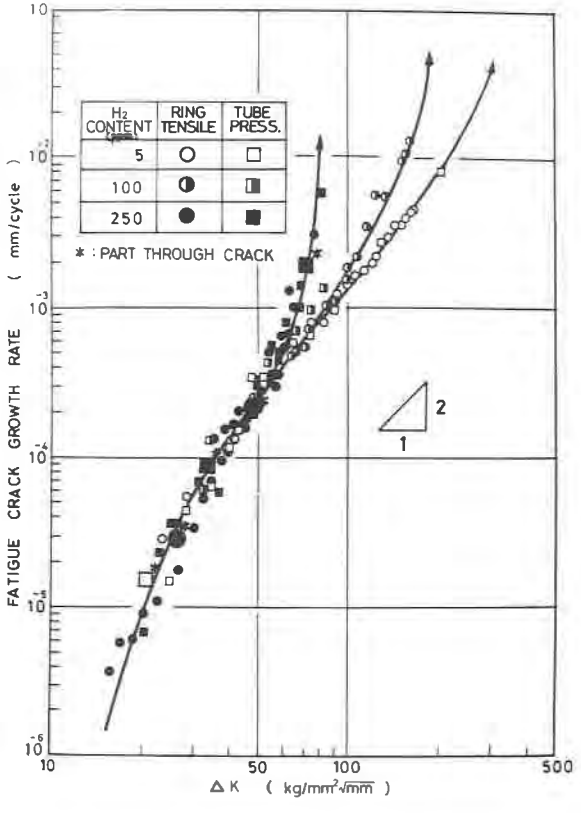

Fig. 15 Effect of Hydrogen Content on Fatigue Crack Growth Rate (tested at room temperature)

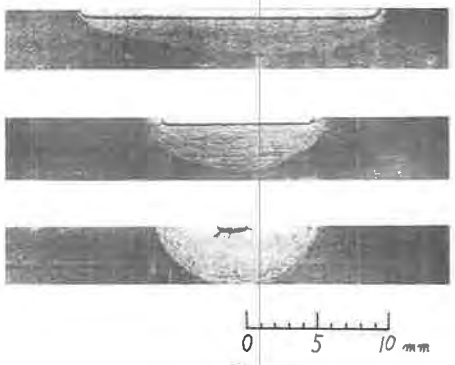

Fig. 16 Examples of Two-Dimensional Fatigue Crack Propagation Behaviour in Ring Tensile Specimen (hydrogen content: 250ppm, $\sigma = 22 \leftrightarrow 2 kg/mm^2$, tested at room temperature)

(a) Tube Pressurizing, $\sigma = 22 \leftrightarrow 2$ kg/mm², Hydrogen Content = 5ppm

(b) Ring Tensile, $\sigma = 22 \leftrightarrow 2$ kg/mm², Hydrogen Content = 250ppm

0 5 mm

Fig. 18 Examples of Two-Dimensional Fatigue Crack Propagation Behaviour at 300°C

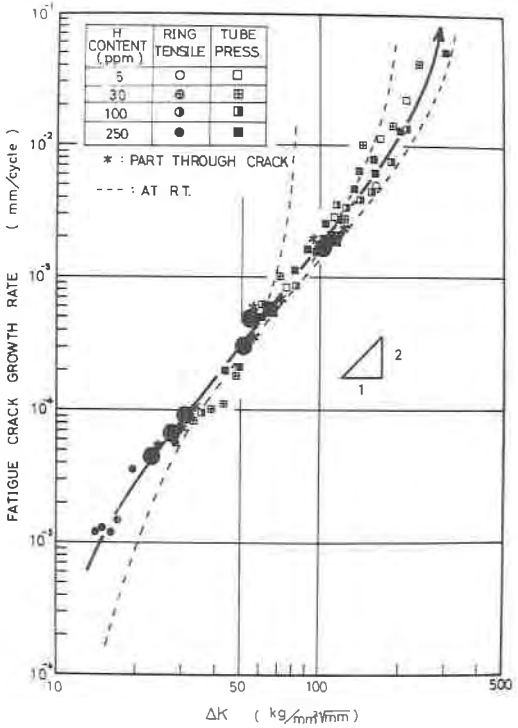

Fig. 17 Fatigue Crack Growth Rate at 300°C